Collective dynamic properties in simple crystals: Influence of the structural disorder

N. Anento and J. A. Padró
Departament de Física Fonamental, Universitat de Barcelona, Diagonal, 647, 08028 Barcelona, Spain
(Received 29 March 2004; revised manuscript received 12 July 2004; published 28 December 2004)

Collective dynamic properties in Lennard-Jones crystals are investigated by molecular dynamics simulation. The study is focused on properties such as the dynamic structure factors, the longitudinal and transverse currents and the density of states. The influence on these properties of the structural disorder is analyzed by comparing the results for one-component crystals with those for liquids and supercooled liquids at analogous conditions. The effects of species-disorder on the collective properties of binary crystals are also discussed.

DOI: 10.1103/PhysRevB.70.224211 PACS number(s): 61.25.Bi, 05.60.Cd

I. INTRODUCTION

Molecular dynamics (MD) simulation is a powerful tool to investigate the properties of condensed matter at an atomic level. MD has been extensively applied to the study of the structure and dynamics of disordered systems as liquids and glasses, which can be hardly analyzed by using the usual approximations for crystalline systems. The study of the atomic dynamics in liquids is usually based on the calculation of time correlation functions for single particles including the velocity autocorrelation functions and the mean square displacements. However, interesting information on the dynamic behavior may also be obtained through collective properties such as the dynamic structure factors, the longitudinal and transverse current spectra and corresponding dispersion curves.[1] The collective dynamic properties in one-component liquids were largely studied[2] whereas binary liquid mixtures have been the subjects of recent investigations (see, for example[3] and references therein). The influence of local order on the collective dynamic properties of some liquids with an incipient short-ranged structure, such as molten salts, was already discussed.[3,4] Some features of the collective dynamic properties in solids and the influence of structural and chemical order will be discussed in this paper.

From a theoretical point of view the dynamic properties of ordered phases are normally based on approximate calculations. The most frequent approach to the lattice dynamics is based on the assumption of an harmonic interaction of each atom with their nearest neighbors (i.e. the elastic energy is a function of their relative displacements). This approach, which takes advantage of the long-range periodicity of the crystal lattices, was established prior to the development of the computer simulation methods and produced valuable results such as the introduction of normal modes and phonons to analyze the dynamical behavior of crystals.[5] Thus, the use of MD simulation methods is not imperative for the study of ideal crystalline solids but they become essential to analyze the structure and dynamics of the defects in crystal lattices.[6,7] Although the same procedures used for disordered systems may be applied to ordered crystals the MD analyses of the collective dynamic properties for these systems are rather scarce and to our knowledge reduced to an early study of longitudinal modes in rare gas solids.[8]

Our aim in this paper is to improve our understanding on the basis of the dynamical behavior of condensed systems at an atomic level. The differences between solids and liquids are analyzed paying special attention to the influence of the structural atomic disorder on the collective dynamic properties. To this end, the properties obtained for a one-component Lennard-Jones crystal are compared with those for a structurally disordered system at analogous conditions (the same density and temperature). The same potential model was used in all the simulations. For the sake of completeness the dynamic collective properties in binary crystals are also analyzed and the influence of chemical disorder is investigated by comparing the results for a completely ordered binary crystal and those for a binary crystal with particles of distinct species randomly distributed.

II. DESCRIPTION OF THE SIMULATED SYSTEMS

Computer simulations of systems made up of N atoms were performed according to the ordinary MD method and considering usual periodic boundary conditions.[1] A leapfrog Verlet algorithm with coupling to a thermal bath[9] and a time-step $\Delta t = 5$ fs was used for the integration of the equations of motion. Two kinds of systems were simulated.

One-component systems (Ne). Four systems made up of Ne atoms at the same atomic density $\rho = 4.5667 \times 10^{-2}$ Å^{-3} were simulated (NVT simulations) by assuming the same 12-6 Lennard-Jones potential ($\varepsilon = 42$ K, $\sigma = 2.755$ Å)

(i) Two fcc crystals at $T = 5$ K and $T = 20$ K that will be termed C5 and C20, respectively. The lattice constant at this density is $a = 4.44$ Å and the corresponding nearest-neighbor distance is 1.14σ. The initial configuration was generated by locating Ne atoms with random velocities (according to the given temperature) at the lattice points of a fcc structure. The k-dependent dynamic properties of these systems were calculated for wavevectors along the (1,0,0), (1,1,0) and (1,1,1) directions and modulus ranging from $k = 0.177$ Å^{-1} to $k = 2.001$ Å^{-1}. Since the lowest wavevector that may be analyzed from a MD run depends on the size of the simulated system we have carried out MD runs with either $N = 864$ or $N = 2048$. The agreement between the calculated properties for the two systems at close wavevectors have shown that the results are not significantly influenced by the size of the simulated system.

(ii) Two disordered sets. The former (L40) was ordinary liquid Ne at $T = 40$ K. To generate the initial configuration

the temperature of the C40 system was increased up to $T=80$ K. After checking that the system was in a liquid phase it was cooled up to $T=40$ K. During these processes the density of the system was kept constant. The second disordered system was obtained by a fast cooling of the L40 liquid up to $T=20$ K at constant density. The resulting system, which shows the characteristic features of a glassy system (disordered structure and very low diffusivity), will be termed G20. The k-dependent dynamic properties for these disordered systems were calculated for wavevectors with the same modulus as those for the crystals.

Binary crystals ($Ne_{0.5}$-$He_{0.5}$). A procedure analogous to that used for one-component systems was applied to simulate $Ne_{0.5}$-$He_{0.5}$ at an atomic density $\rho=4.9572\times10^{-2}$ Å^{-3} and temperature $T=20$ K. The potential parameters for He were $\varepsilon=10$ K and $\sigma=2.602$ Å and the ordinary Lorentz-Berthelot rules[1] were assumed for the interactions between unlike particles. The method for the calculation of the collective dynamic properties is the same as in recent MD studies of binary liquid mixtures (see Ref. 3 and references therein). Two systems that only differ in their internal chemical order were considered.

(iii) In the ordered binary crystal (OBC) the atoms of different species were alternatively located in the sites of the fcc pattern whereas in the disordered binary crystal (DBC) the atoms of distinct species were randomly distributed in the fcc lattice (the resulting structures will be commented on in Sec. IV).

In all cases the dynamic collective properties were calculated during production MD runs of 10^5 time-steps after equilibration periods of 4×10^4 time-steps. Since some of the simulated systems could be at unstable states it was verified that the state of the system, which was characterized by its structure $[g(r)]$ and self-diffusion coefficient (D), was the same prior and after the production MD runs for the calculation of collective properties. This is especially important in the case of the L40 and G40 systems, which temperature and density correspond to the fluid-solid region of the phase diagram.[10] In the case of both one-component and binary crystals the test is easier since there is not diffusion and atoms would remain at the same lattice points as in the initial configuration.

III. RESULTS FOR THE ONE-COMPONENT SYSTEMS

A. Structure and single dynamic properties

As may be observed in Fig. 1 the radial distribution function $[g(r)]$ for C5 shows very well defined peaks at all the characteristic distances of a fcc structure. These peaks become lower and wider as temperature increases so that some of them are almost indiscernible for C20. In contrast, the $g(r)$'s for both L40 and G20 show the typical shapes of these functions for dense liquids. The peaks of the $g(r)$ are located at very close positions for the two systems but the maximums and minimums are somewhat less marked for L40. The $g(r)$ results corroborate that the structure of C20 keeps the main features of a typical crystal and it shows large differences in relation to the disordered structure of the super-

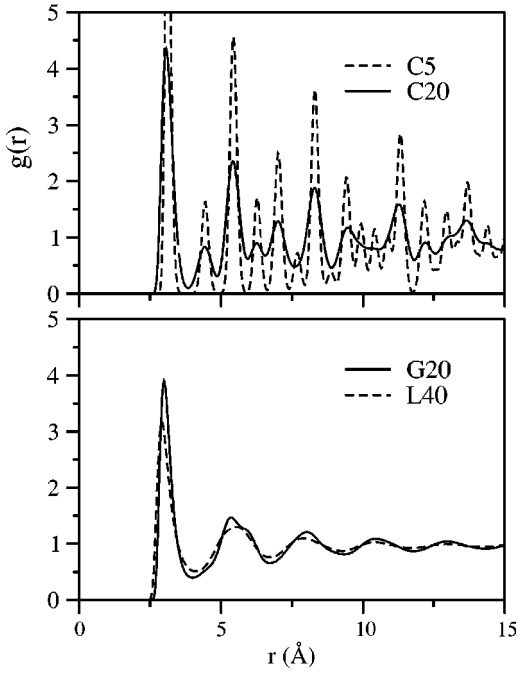

FIG. 1. Radial distribution functions.

cooled liquid G20 that looks like those of simple dense liquids.

The self-diffusion coefficients were obtained from the slope of the mean square displacements $[r^2(t)]$ shown in Fig. 2(a). In the case of the crystals C5 and C20 the $r^2(t)$ results corroborate the nondiffusive behavior of the atoms in these systems. The D coefficient for the liquid L40 is $D=7.9\times10^{-6}$ cm^2 s^{-1}, which is a typical value for dense liquids,[1] whereas for G20 is one order of magnitude lower ($D=5.1\times10^{-7}$ cm^2 s^{-1}). Thus from a single dynamics point of view the behavior of G20 is analogous to that of solids (at least for the rather short time intervals that may be simulated by MD), which corroborates that G20 can be taken as representative of glassy systems. It should be noted that the interatomic potential as well as the temperature and density of C20 and G20 is the same while their atomic mobility is rather close, being the most outstanding difference between them the structural order. Therefore, a systematic comparison of the results for C20 and G20 is a suitable way to analyze the influence of the disorder on the collective dynamic properties.

The normalized velocity autocorrelation functions $[C(t)=\langle\mathbf{v}(t)\cdot\mathbf{v}(0)/v^2(0)\rangle]$ were calculated during the MD simulations from the time evolution of the atomic velocities. The results are shown in Figs. 2(b) and 2(c). The $C(t)$ functions for the C5 and C20 crystals show an oscillatory behavior and a very deep first minimum with both the minimum and the oscillations more pronounced for the system at lower temperature. The shape of the $C(t)$ for both L40 and G20 is very different and shows the characteristic trends of the $C(t)$ for liquids. These $C(t)$ functions show a first minimum markedly shallower than that for the C5 and C20 crystals followed by a slight shoulder and no oscillations. Notice the similarity between the shape of $C(t)$ for L40 and G20 despite their time

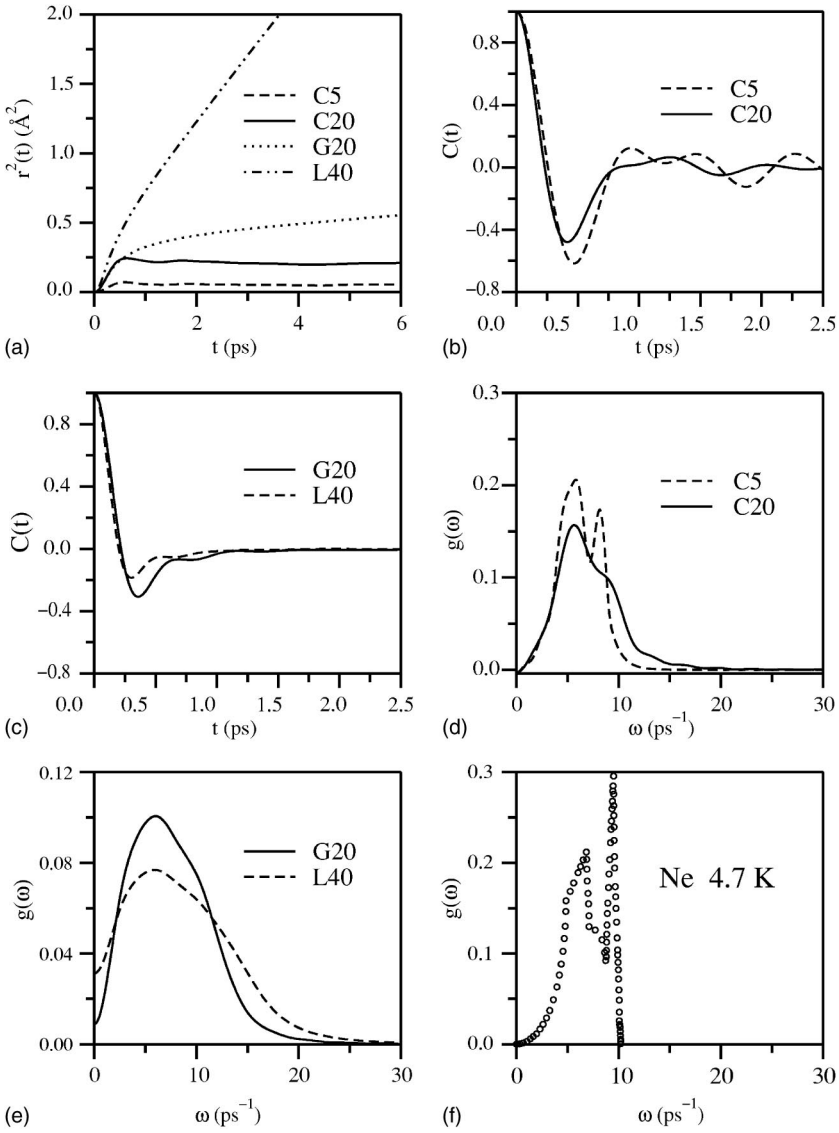

FIG. 2. Mean square displacements (a). Velocity autocorrelation functions (b) and (c). Density of states (d) and (e). Density of states obtained through the Born-von Kármán model and experimental dispersion curves (Ref. 15) (f).

integrals [and therefore $r^2(t)$ and D] are very different. On the contrary there are large differences between the $C(t)$ shapes for C20 and G20 despite the fact both systems show a low atomic mobility.

To analyze the single particle dynamics it is interesting to calculate the densities of states $g(\omega)$, which are obtained by Fourier transforming the $C(t)$ functions. The resulting $g(\omega)$ curves that are shown in Figs. 2(d) and 2(e) were calculated according to the normalization condition $\int g(\omega)d\omega=1$. The $g(\omega)$ curves for C5 show two marked peaks, which are the characteristic features of these functions for crystals. The low-frequency peak is mainly associated with the transverse modes whereas the high frequency peak is associated with the longitudinal modes.[11,12] As T increases the peaks become smoothed and the high-frequency peak for C5 appears as a shoulder for C20. In the case of liquids the two peaks cannot be distinguished by observing the shape of the $g(\omega)$ curves but it was shown that the low and high frequency regions of $g(\omega)$ should be also related to the contributions of the transverse and the longitudinal modes, respectively.[13,14] From the comparison of the $g(\omega)$ for C20 and G20 in Fig. 2 it is clear that the structural disorder produces overlapping of the frequencies corresponding to the longitudinal and transverse modes and only one frequency band is visible in $g(\omega)$ of liquids.

The density of states $g(\omega)$ is one of the properties ordinarily considered in the theoretical treatments of solid crystals. $g(\omega)$ for Ne at 4.7 K was calculated by assuming a two-neighbor Born-von Kármán model and using the experimental dispersion curves.[15] The resulting $g(\omega)$ is shown in Fig. 2(f). As may be observed by comparing Figs. 2(d) and 2(f) the $g(\omega)$ function calculated by MD for the C5 system shows an overall accordance with that obtained through experimental data. Both $g(\omega)$ functions show two marked peaks at quite close positions though some quantitative discrepancies, such as the different height of the second peak and the lack of a high frequency tail in the "experimental" $g(\omega)$, may be observed. It should be emphasized that the "experimental" $g(\omega)$ was not obtained from direct measurements but assuming a simple model.

The interpretation of the $g(\omega)$ results in hydrogen bonded liquids (as water) has recently been the subject of

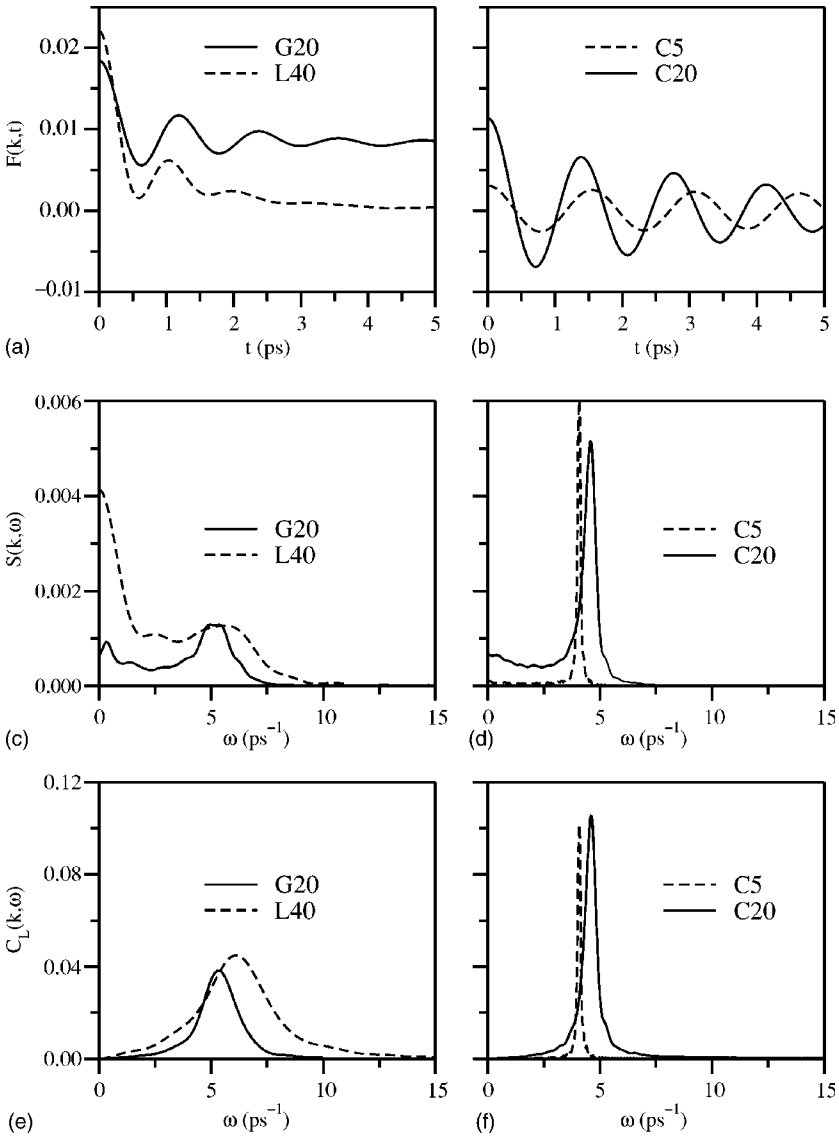

FIG. 3. MD results at $k = 0.41$ Å^{-1}. Intermediate scattering functions (a) and (b); dynamic structure factors (c) and (d); longitudinal current spectra (e) and (f).

discussion.[12,16,17] The $g(\omega)$ curves for these systems show two peaks. A low frequency peak that is a characteristic feature of $g(\omega)$ for all sorts of dense liquids and has been attributed to the frustrated translations due to the local structure around a given atom (or molecule) that produces a cage effect. A high frequency peak that cannot be observed in the $g(\omega)$ of no associated liquids and has been related to the stretching motions of hydrogen bonded molecules along the bond direction.[16] This interpretation of the microscopic origin of these bands has been partially criticized by De Santis *et al.*,[12] which suggest that the two bands are present in all liquids including no associated liquids. The arguments given by De Santis *et al.* were mainly based on the existence of two bands in the $g(\omega)$ curves for solid Ar at 20 K and quenched amorphous water at 70 K. However, our results show that the high frequency band becomes weakened as temperature increases and is not visible in disordered systems. Then, the high frequency peak in $g(\omega)$ for liquids is only visible in liquids with a local structure that favors the existence of longitudinal modes associated to motions such as the hydrogen bond stretching in water.[17]

B. Longitudinal modes

The intermediate scattering functions $F(k,t)$, which are defined as the time correlations of the density fluctuations,[1] were calculated for different wavenumbers from the atomic trajectories obtained during the MD simulations. The time spectra of the $F(k,t)$ functions are the dynamic structure factors $S(k,\omega)$, which are directly related to measurements of coherent inelastic scattering of thermal neutrons with wavelengths around the interatomic distances.

In general, $F(k,t)$ for a given wavenumber k shows a decaying oscillatory behavior. In the case of liquids such as L40, $F(k,t)$ at small k shows noticeable oscillations and a relatively fast decay [see the results for $k=0.41$ Å^{-1} in Fig. 3(a)]. Thus $S(k,\omega)$ has a relaxation peak centered at $\omega=0$ (Rayleigh peak) that represents a thermal diffusive (nonvibrational) mode and two side peaks at $\omega=\pm ck$ (Brillouin peaks) that reflect the oscillatory behavior of $F(k,t)$. The Brillouin peaks correspond to vibrational modes related to acoustic waves propagating with isothermal sound velocity c. The behavior of $F(k,t)$ for the glass system G20 is similar

to that for liquids but shows a slower time decay that does not allow a straightforward calculation of $S(k,\omega)$. Thus, to determine the $S(k,\omega)$ spectra for this system [Fig. 3(c)] the corresponding $F(k,t)$ functions were vertically shifted [$\Delta F(k,t)\approx -0.009$ for $k=0.41$ Å^{-1} in Fig. 3(a)]. It should be noticed that the Brillouin peaks for L40 and G20 at different wavenumbers are located at rather close positions but the $S(k,\omega)$ functions at low frequencies show marked differences since the outstanding Rayleigh peaks for L40 are almost absents for G20, as corresponds to the lack of thermal diffusion in the last system.

In the case of crystals the oscillatory contributions to $F(k,t)$ are dominant [Fig. 3(b)]. The absence of diffusive contributions is reflected in the $S(k,\omega)$ spectra for C5 and C20 [Fig. 3(d)], which do not show the Rayleigh peak whereas a very well defined Brillouin peak has been found for all the analyzed wavenumbers. Because of the anisotropy of the C5 and C20 crystals, the dynamic collective properties depend on the direction of the wavevectors. Thus the $F(k,t)$ functions and their $S(k,\omega)$ spectra for the wavevectors corresponding to the (1,0,0), (1,1,0) and (1,1,1) directions were calculated separately. The dispersion relations $\omega(k)$ for three directions were then obtained separately from the positions of the corresponding Brillouin peaks of $S(k,\omega)$.

The dynamic structure factor $S(k,\omega)$ is a microscopic property of crystals available from neutron scattering experiments. The frequencies associated at each wavelength may be obtained and the corresponding dispersion curves determined. The results from neutron scattering experiments for Ne at 5 K[15] are shown in Fig. 4. For the sake of comparison the MD findings for the C5 and C20 crystals found in this study have been represented in the same form as the experimental findings in Ref. 15 and the results are also shown in Fig. 4. Though the frequencies for C5 are somewhat lower than those from experiment a good accordance may be observed between the MD results and experimental findings. This supports the fact that the computer simulation results for simple crystals in this study may be taken as representative of the behavior of actual systems. As expected, the $\omega(k)$ curves for C5 and C20 reflect that the frequency for a given k increases with temperature.

To study the longitudinal modes it is useful to consider the longitudinal current correlation functions $C_L(k,\omega)$, which are related to $S(k,\omega)$ according to $C_L(k,\omega)=(\omega/k)^2 S(k,\omega)$.[1] Thus $C_L(k,\omega)$ for liquids do not show a maximum at $\omega=0$ and the peak at high frequency is enhanced, becoming much more marked than the corresponding one in $S(k,\omega)$ [see $S(k,\omega)$ and $C_L(k,\omega)$ for L40, Fig. 3]. Though the information provided by $C_L(k,\omega)$ and $S(k,\omega)$ is in principle the same,[18] $C_L(k,\omega)$ does not show the thermal diffusive contribution of the density fluctuations [i.e. the Rayleigh peak of $S(k,\omega)$ at $\omega=0$] whereas the contribution of the vibrational modes of density fluctuations is highlighted. It should be noted that the $F(k,t)$ functions for disordered systems frequently show long time tails for some wavevectors and then the $S(k,\omega)$ cannot be accurately determined. However, this problem does not appear in the calculation of $C_L(k,\omega)$ since the time decay of $C_L(k,t)$ is in general quite fast. A dispersion relation $\omega_L(k)$ may be determined from the peaks of the

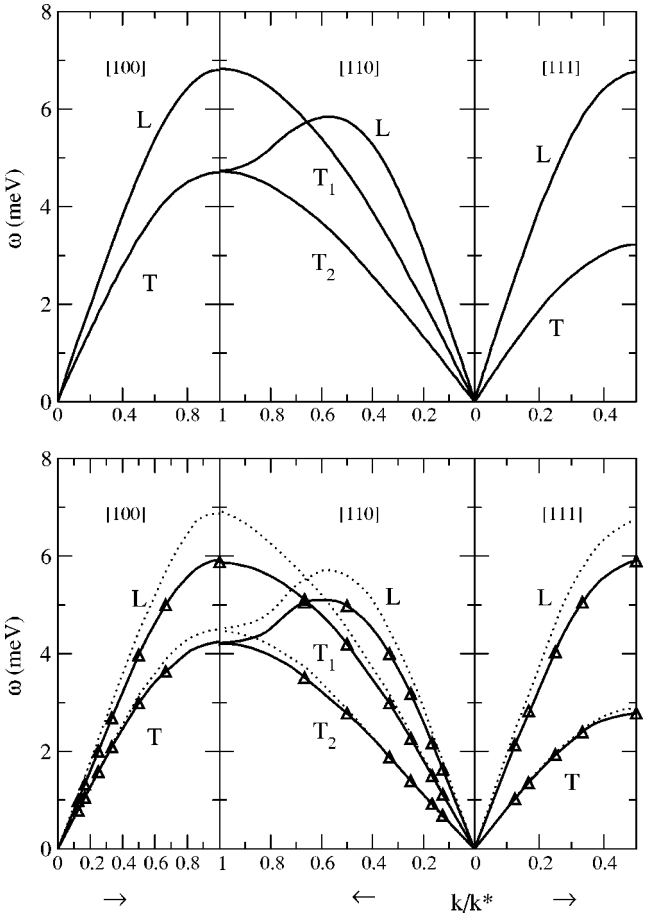

FIG. 4. Phonon dispersion curves from neutron scattering experiments for Ne at 5 K (Ref. 15) (upper frame) and those obtained in this work (lower frame). Triangles and the interpolating continuous line are the MD results for C5. The dotted line corresponds to the MD results for C20.

$C_L(k,\omega)$ functions. According to (1), the frequency corresponding to the Brillioun peak of $S(k,\omega)$ for a given k should be slightly lower than the one corresponding to the $C_L(k,\omega)$ peak for the same k (see Fig. 3) and then $\omega(k)\leqslant\omega_L(k)$. However, these differences decrease with k and should vanish at the hydrodynamic limit ($\omega\to 0$). In the case of solids the diffusive contributions are absent and the time spectra of the $F(k,t)$ functions can be then calculated without important problems. Nevertheless, for the sake of comparison, we have also determined the $C_L(k,\omega)$ functions for C5 and C20.

The $C_L(k,\omega)$ functions for C20 and G20 at several representative wavenumbers are compared in Fig. 5. As a general rule we can say that the peaks of $C_L(k,\omega)$ are located at rather similar positions for the two systems but the most outstanding difference is that they are markedly wider for the glass. These facts are clearly reflected in Fig. 6. We cannot observe significant discrepancies between the longitudinal dispersion curves $\omega_L(k)$ for C20 and G20 being $\omega_L(k)$ for the glassy system intermediate between those along the three directions of the crystal. We also estimated the damping coefficients $\Gamma(k)$ obtained as the half width at half maximum of the $C_L(k,\omega)$ peaks. These coefficients give us information

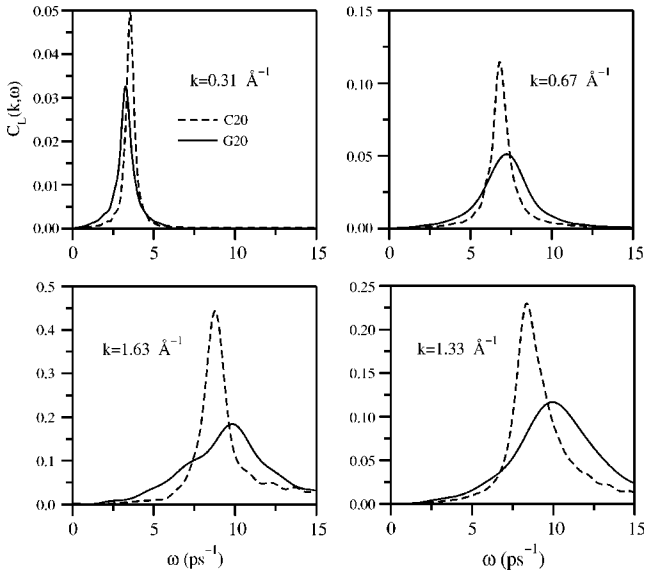

FIG. 5. Longitudinal current spectra for C20 and G20 at different wavenumbers.

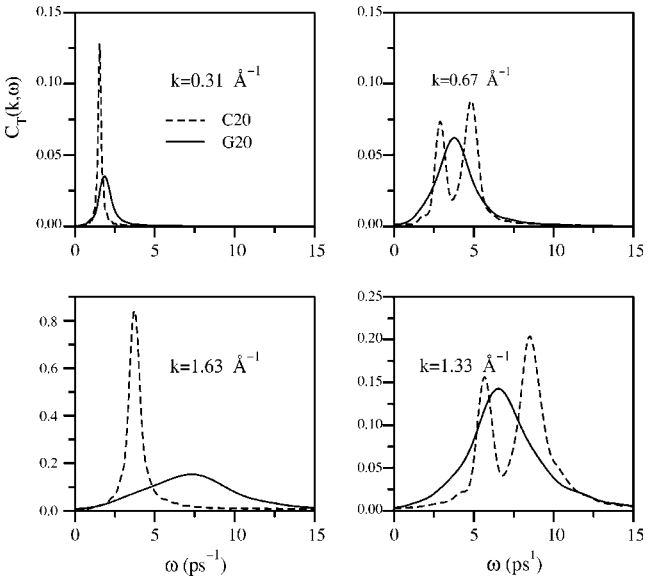

FIG. 7. Transverse current spectra for C20 and G20 at different wavenumbers.

about the lifetimes of the corresponding modes. According to the results plotted in Fig. 6 the $\Gamma(k)$ values of the damping are markedly higher for G20 than for C20 at all directions. Findings in Figs. 5 and 6 corroborate that the structural disorder has no significant influence on the values of the characteristic frequencies of longitudinal modes but produces a substantial decrease in the lifetimes of these modes. According to these findings the adiabatic sound velocity v_s (calculated as the slope of the dispersion curve at low wavenumbers $v_s=\omega_L/k$) is little influenced by the disorder and the well known differences of v_s for solids and liquids should be mainly attributed to the differences in density and temperature but not to their different structures.

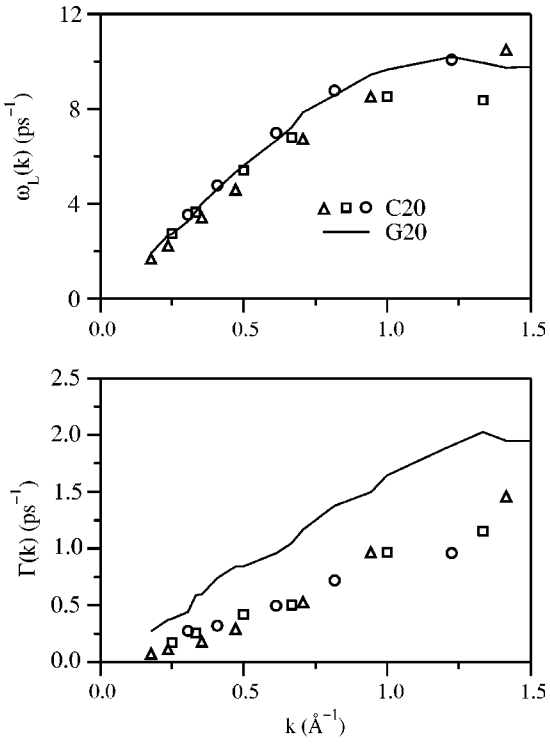

FIG. 6. Longitudinal dispersion curves (upper frames) and damping coefficients (lower frames). Results for G20 (continuous line) and for C20 along the (1,0,0) (triangles), the (1,1,0) (squares) and the (1,1,1) (circles) directions.

The anisotropy of the crystals is clearly shown by the longitudinal dispersion curves $\omega_L(k)$ obtained for C20 (Fig. 6). Though the differences between the $\omega_L(k)$ findings along the three considered directions are not very large, it may be observed that v_s for wavevectors along (1,1,1) is somewhat higher than that along (1,0,0) whereas v_s along (1,1,0) is intermediate. These findings are in agreement with the data from experiments.[15] We have not found any significant dependence of the $\Gamma(k)$ coefficients on the wavevector direction (see Fig. 6).

C. Transverse modes

Information on collective dynamics is also provided by the transverse current correlation functions $C_T(k,t)$ and corresponding spectra $C_T(k,\omega)$, which are related to the existence of propagating shear modes. In the case of liquids $C_T(k,\omega)$ cannot be directly associated with any measurable quantity and may be only determined from MD "computer experiments." However, it is well known that $C_T(k,\omega)$ for liquids show a maximum at finite wavevectors ($k>k_t$) that should be associated with the propagation of transverse modes due to viscoelastic effects.[1,2]

As with longitudinal modes, the transverse dispersion curves obtained from MD are in good accordance with those from the experiment[15] (see Fig. 4). The $C_T(k,\omega)$ functions for the C5 and C20 crystals corresponding to wavevectors along the (1,1,0) directions show two well defined peaks (Fig. 7). Then, in accordance with the experimental findings (Fig. 4) two dispersion curves are obtained for the modes in

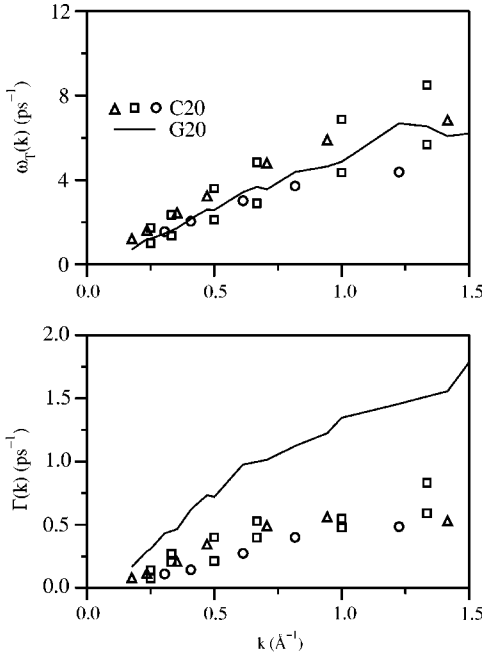

FIG. 8. Transverse dispersion curves (upper frames) and damping coefficients (lower frames). Results for G20 (continuous line) and for C20 along the (1,0,0) (triangles), the (1,1,0) (squares) and the (1,1,1) (circles) directions.

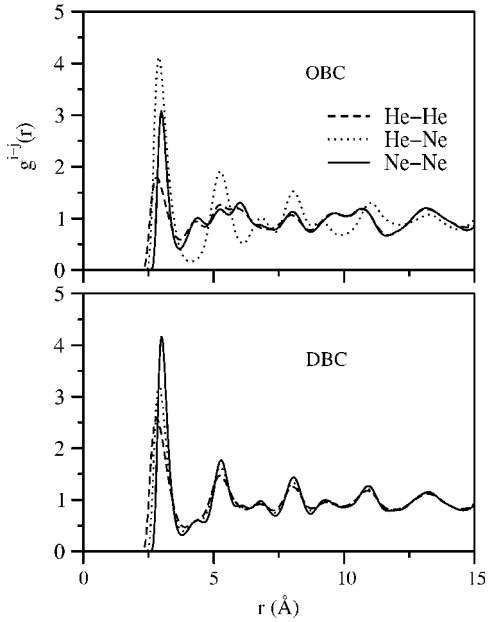

FIG. 9. Partial radial distribution functions of the simulated binary crystals.

this direction. The upper curve is very close to that corresponding to the (1,0,0) direction whereas the lower curve is very close to that for the (1,1,1) direction (Fig. 8).

The $C_T(k,\omega)$ functions for C20 at several representative wavenumbers are compared with the ones for G20 in Fig. 7. The differences between the $C_T(k,\omega)$ results for the two systems are larger than those found for $C_L(k,\omega)$, especially in the case of the functions with a double peak. The dispersion curve associated with the transverse modes in the disordered system G20 is intermediate between the two curves for the crystal (Fig. 8), which shows that the frequencies associated with these modes are not significantly influenced by the structural disorder. However, as with longitudinal modes the damping coefficients for G20 are markedly higher (and the lifetimes markedly lower) than the corresponding ones for C20 (Fig. 8). Moreover, the dispersion relation for G20 show a liquid-like behavior at small wavenumbers and, unlike for the C5 and C20 crystals along the three directions, it goes to a finite ω-value as k goes to zero.

IV. RESULTS FOR THE BINARY CRYSTALS

A. Structure and single dynamic properties

The initial configurations of the ordered binary system (OBC) were made up of two cubic structures of Ne atoms an two cubic structures of He atoms suitably shifted to obtain a fcc structure with the two species symmetrically distributed. Thus, as shown in Fig. 9, the resulting partial radial distribution functions for the like atoms [$g^{\mathrm{NeNe}}(r)$ and $g^{\mathrm{HeHe}}(r)$] in the OBC system are very close and only show significant differences at short distances. The discrepancies in the first maximum should be attributed to the differences in the interaction potential that should be mainly associated with the different size of the atoms of the two species. In the disordered binary system (DBC) the atoms of different species were initially located at random to occupy all the sites of an fcc structure. Then the three partial radial distribution functions $g^{\mathrm{NeNe}}(r)$, $g^{\mathrm{NeHe}}(r)$ and $g^{\mathrm{NeNe}}(r)$ are quite close, which corroborates that the atoms of distinct species are randomly distributed (see Fig. 9).

The density of states for the Ne atoms $g^{\mathrm{Ne}}(\omega)$ and the He atoms $g^{\mathrm{He}}(\omega)$ for the OBC and DBC systems are shown in Fig. 10. It is clear that the spectrum of frequencies associated with the lighter He atoms is wider and shifted towards higher ω-values than that for the Ne atoms. The influence of the species disorder on $g^{\mathrm{Ne}}(\omega)$ and $g^{\mathrm{He}}(\omega)$ is rather weak. Moreover, $g^{\mathrm{Ne}}(\omega)$ for OBC is very similar to that for the one-component system (Fig. 2) though the frequency corresponding to the peak of $g^{\mathrm{Ne}}(\omega)$ for OBC is slightly lower than that for C20. It should be noted that the weak shoulder in $g^{\mathrm{Ne}}(\omega)$ for OBC cannot be observed for DBC, which is consistent with the findings for the one-component systems where the shoulder also tend to disappear with the disorder.

B. Longitudinal modes

To study the collective dynamic properties in multicomponent systems one can calculate the partial longitudinal current correlation functions [$C_L^{\mathrm{NeNe}}(k,t)$, $C_L^{\mathrm{HeHe}}(k,t)$ and $C_L^{\mathrm{HeNe}}(k,t)$] defined according to the usual definitions[1,2] and the corresponding time spectra [$C_L^{\mathrm{NeNe}}(k,\omega)$, $C_L^{\mathrm{HeHe}}(k,\omega)$ and $C_L^{\mathrm{HeNe}}(k,\omega)$]. The peaks of these spectra allow us to obtain the characteristic frequencies of each species for a given wavenumber. The partial longitudinal dispersion curves for the Ne and He subsystems [$\omega_L^{\mathrm{Ne}}(k)$ and $\omega_L^{\mathrm{He}}(k)$] obtained for the OBC and DBC systems are shown in Fig. 11. It is also

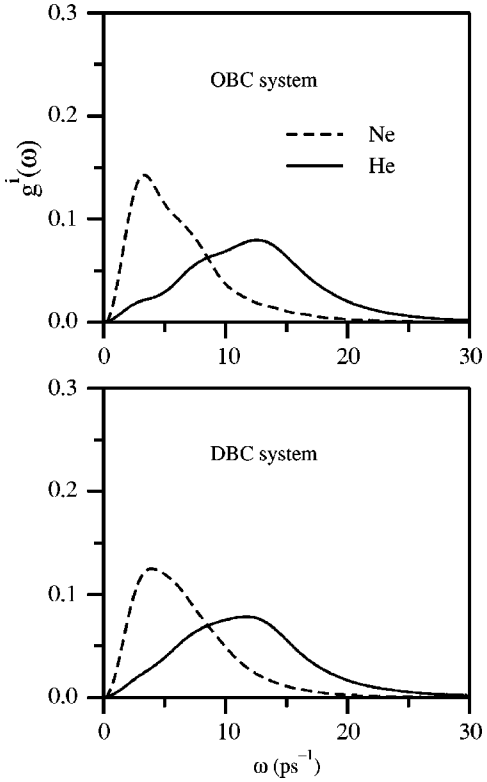

FIG. 10. Density of states for both Ne and He atoms

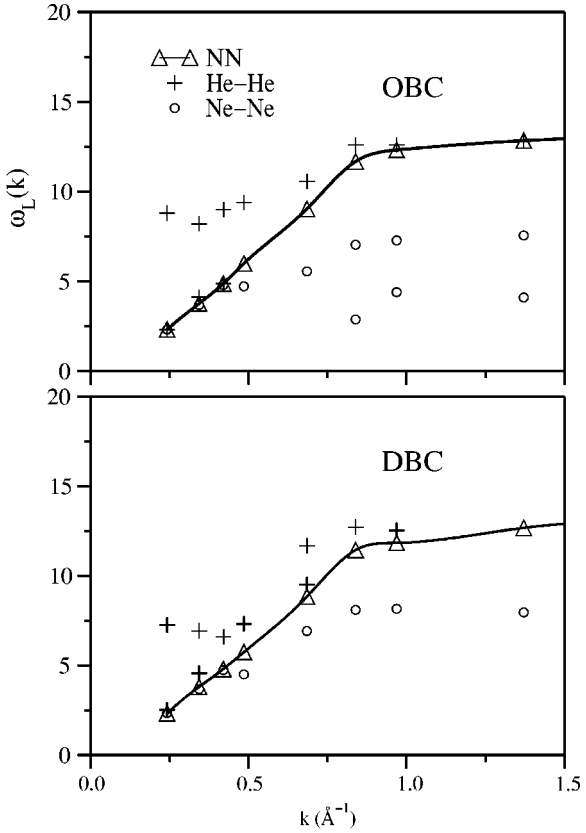

FIG. 11. Longitudinal dispersion curves obtained from the positions of the peaks in the $C_L^{\mathrm{NN}}(k,\omega)$, $C_L^{\mathrm{NeNe}}(k,\omega)$ and $C_L^{\mathrm{HeHe}}(k,\omega)$ spectra.

useful to consider the number density longitudinal current correlation spectrum $C_L^{\mathrm{NN}}(k,\omega)$ that reflects the averaged behavior of the mixture. For binary systems $C_L^{\mathrm{NN}}(k,\omega)$ is defined as[19]

$$C_L^{\mathrm{NN}}(k,\omega) \equiv x_{\mathrm{Ne}} C_L^{\mathrm{NeNe}}(k,\omega) + x_{\mathrm{He}} C_L^{\mathrm{HeHe}}(k,\omega) + 2(x_{\mathrm{Ne}} x_{\mathrm{He}})^{1/2} C_L^{\mathrm{HeNe}}(k,\omega). \quad (1)$$

Recent MD studies of liquid binary mixtures[18,20] have shown that, for a given k, the frequency associated with the light particles is in general higher than that for the heavy particles. However, for wavenumbers smaller than a given value (hydrodynamic regime) the frequencies for the light and heavy particles become equal so that $\omega_L^{\mathrm{Ne}}(k) = \omega_L^{\mathrm{He}}(k) = \omega_L^{\mathrm{NN}}(k)$. As may be observed in Fig. 11 these relations are also fulfilled for crystals and the three relation dispersions are coincident at low frequencies. It should be noted that at low k-values the $C_L^{\mathrm{HeHe}}(k,\omega)$ spectra for both the OBC and DBC systems show two peaks. One of them corresponds to the same frequency than that for $C_L^{\mathrm{NN}}(k,\omega)$, whereas the frequency of the other is markedly higher. These high-frequency peaks for light particles were also observed in the case of liquid mixtures being initially associated with the existence of "fast sound" propagating modes.[21] However, a careful analysis of the origin of these peaks has shown that they should be attributed to the existence of modes of kinetic character analogous to the optic modes in ionic mixtures.[4,20,22,23] After the initial regime the qualitative features of the number density and partial relation dispersion are analogous to those for binary liquids,[4,18,20] i.e. $\omega_L^{\mathrm{He}}(k) \approx \omega_L^{\mathrm{NN}}(k)$ and $\omega_L^{\mathrm{Ne}}(k) < \omega_L^{\mathrm{NN}}(k)$.

Moreover, it should be noticed that $C_L^{\mathrm{NeNe}}(k,\omega)$ for the OBC system show a second peak. These low-frequency modes of kinetic character become damped with disorder and do not appear in the $C_L^{\mathrm{NeNe}}(k,\omega)$ spectra for DBC.

C. Transverse modes

The partial transverse current spectra $C_T^{\mathrm{HeHe}}(k,\omega)$, $C_T^{\mathrm{NeNe}}(k,\omega)$ and $C_T^{\mathrm{HeNe}}(k,\omega)$ were also obtained from the MD runs as the time Fourier transforms of the partial transverse current correlation functions defined according to the usual definitions.[1,2] The corresponding number density transverse current spectra $C_T^{\mathrm{NN}}(k,\omega)$ were then calculated according to Eq. (1).[19,24]

As with longitudinal modes for wavenumbers smaller than a given value the frequencies of the light and heavy particles for both OBC and DBC become equal so that $\omega_T^{\mathrm{Ne}}(k) = \omega_T^{\mathrm{He}}(k) = \omega_T^{\mathrm{NN}}(k)$ (Fig. 12). Moreover, the $C_T^{\mathrm{HeHe}}(k,\omega)$ spectra show two peaks: one at the same frequency as that for $C_T^{\mathrm{NN}}(k,\omega)$ and the other, which should associate with modes of kinetic character, at a higher frequency. These findings are qualitatively similar to those found for binary liquid mixtures of moderately different masses.[24] It should be noted that the existence of low frequency kinetic modes are associated to the heavier Ne atoms for both the OBC and DBC

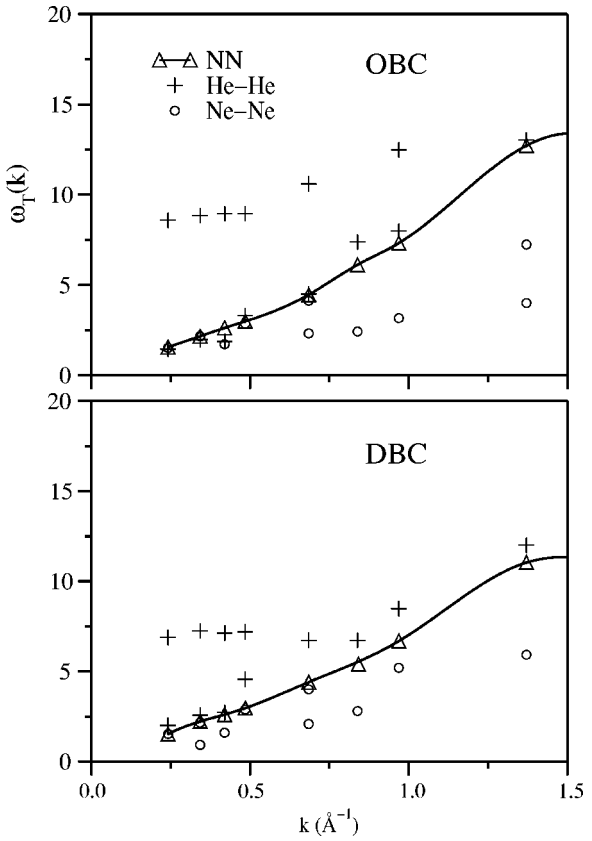

FIG. 12. Transverse dispersion curves obtained from the positions of the peaks in the $C_L^{\mathrm{NN}}(k,\omega)$, $C_L^{\mathrm{NeNe}}(k,\omega)$ and $C_L^{\mathrm{HeHe}}(k,\omega)$ spectra.

systems. In general, we can say that solid mixtures show more transverse kinetic modes than liquid mixtures.

V. CONCLUDING REMARKS

The longitudinal and the transverse dispersion relations as well as the density of states for solid Ne resulting from the MD calculations with a Lennard Jones potential show an overall accordance with those obtained through experiments. This supports that computer simulation findings for simple crystals in this study may be taken as representative of the behavior of actual systems.

The density of states for crystals shows two characteristic features. A low frequency peak mainly associated with transverse modes and a high frequency peak related to the longitudinal modes. As T increases the peaks become smoothed and the high-frequency peak becomes a shoulder so that in the case of liquids the two peaks cannot be distinguished. A comparison of the results for a crystal and a supercooled liquid at the same temperature shows that the structural disorder produces overlapping of the frequencies corresponding to the longitudinal and the transverse modes. This is consistent with earlier findings,[16,17] which suggested that the high frequency peak in the spectral density for liquids is only visible in systems with a local structure that favors the existence of longitudinal modes associated to specific motions (i.e. the intermolecular stretching motions of hydrogen bonded molecules in water).

According to the results in this study the structural disorder has no significant influence on the values of the characteristic frequencies of both longitudinal and transverse modes but produces a substantial decrease in the lifetimes of these modes. So, the adiabatic sound velocity v_s (calculated as the slope of the longitudinal dispersion curve at low wavenumbers $v_s=\omega_L/k$) is little influenced by the disorder and the well known differences of v_s for solids and liquids should be mainly attributed to the differences in density and temperature but not to their different structures. The anisotropy of the crystals is clearly reflected by the relation dispersion obtained in this paper. Though the differences between the longitudinal dispersions along the three considered directions are not very large, v_s for wavevectors along (1,1,1) is somewhat higher than that along (1,0,0) whereas v_s along (1,1,0) is intermediate, which is consistent with the experimental data. It has not been found any significant dependence of the lifetimes of the modes on the wavevector direction.

In the case of binary crystals the frequencies associated with light and heavy particles become equal for wavenumbers smaller than a given value. This behavior, which was also observed in the case of liquid mixtures (hydrodynamic regime), is shown by both longitudinal and transverse modes. Moreover, it has been observed the existence of high frequency modes in the spectra of the light particles and low frequency modes in the spectra of heavy particles. As with liquid mixtures these modes have a kinetic character. As a general rule we can say that the number of peaks (and therefore visible modes) in the longitudinal and transverse current spectra increases with the structural order and is higher in solid than in liquid mixtures.

ACKNOWLEDGMENTS

The financial supports from the DGICYT of the Spanish government (Grant No. BFM2003-08211-C03-02) and the CIRIT of the "Generalitat de Catalunya" (Grant No. 2001SGR-00222) are gratefully acknowledged.

[1] J. P. Hansen and I. R. McDonald, *Theory of Simple Liquids* (Academic, London, 1986).
[2] U. Balucani and M. Zoppi, *Dynamics of the Liquid State* (Clarendon, Oxford, 1994).
[3] N. Anento, J. A. Padró, O. Alcaraz, and J. Trullàs, Mol. Simul. **29**, 373 (2003).
[4] N. Anento and J. A. Padró, Phys. Rev. E **64**, 021202 (2001).
[5] C. Kittel, *Introduction to Solid State Physics* (Wiley, New York, 1996).
[6] D. Hull and D. J. Bacon, *Introduction to Dislocations*

(Butterworth-Heinemann, Oxford, 2001).
[7] A. Serra, Phys. Status Solidi B **227**, 151 (2001).
[8] J. P. Hansen and M. L. Klein, Phys. Rev. B **13**, 878 (1976).
[9] H. J. C. Berendsen, J. P. M. Postma, W. F. Van Gunsteren, M. A. DiNola, and J. R. Haak, J. Chem. Phys. **81**, 3684 (1984).
[10] J. P. Hansen and L. Verlet, Phys. Rev. **184**, 151 (1969).
[11] R. Stedman, L. Almqvist, and G. Nilsson, Phys. Rev. **162**, 549 (1967).
[12] A. de Santis, A. Ercoli, and D. Rocca, J. Chem. Phys. **120**, 1657 (2004).
[13] T. Gaskell and S. Miller, J. Phys. C **11**, 4839 (1978).
[14] N. Anento, J. A. Padró, and M. Canales, J. Chem. Phys. **111**, 10210 (1999).
[15] B. M. Powell and G. Dolling in *Rare Gas Solids* (Academic 1977), Vol. II, Ch. 15, and references therein.
[16] J. A. Padró and J. Martí, J. Chem. Phys. **118**, 452 (2003).
[17] J. A. Padró and J. Martí, J. Chem. Phys. **120**, 1659 (2004).
[18] N. Anento and J. A. Padró, J. Chem. Phys. **116**, 6159 (2002).
[19] N. H. March and M. P. Tosi, *Atomic Dynamics in Liquids* (MacMillan, London, 1986).
[20] N. Anento and J. A. Padró, Phys. Rev. B **62**, 11 428 (2000).
[21] J. Bosse, G. Jacucci, and W. Schirmacher, Phys. Rev. Lett. **57**, 3277 (1986).
[22] R. Fernández-Perea, M. Alvarez, F. J. Bermejo, P. Verkerk, B. Roessli, and E. Enciso, Phys. Rev. E **58**, 4568 (1998).
[23] E. Enciso, N. G. Almarza, M. A. González, F. J. Bermejo, R. Fernández-Perea, and F. Bresme, Phys. Rev. Lett. **81**, 4432 (1998).
[24] N. Anento and J. A. Padró, Mol. Phys. **99**, 275 (2001).